Neuroscience Letters 650 (2017) 139–145

Contents lists available at ScienceDirect

Neuroscience Letters

journal homepage: www.elsevier.com/locate/neulet

Research article

Evidence for mast cell-mediated zinc homeostasis: Increased labile zinc in the hippocampus of mast-cell deficient mice

Rachel H. Kennedy[a,b,*], Amen Wiqas[c], James P. Curley[a,d]

[a] Department of Psychology, Columbia University, New York, NY, USA
[b] Department of Science, Bard Early College-Manhattan, New York, NY, USA
[c] Department of Psychology, Barnard College, New York, NY, USA
[d] Center for Integrative Animal Behavior, Columbia University, New York, NY, USA

HIGHLIGHTS

- Mast cell deficient mice have higher levels of labile brain zinc than wild type animals.
- Total brain zinc levels remain unchanged.
- Granule cell layer and hilar regions of the dentate gyrus are not significantly different.
- Data support mast cell-mediated zinc homeostasis in hippocampus.

ARTICLE INFO

Article history:
Received 24 March 2017
Accepted 20 April 2017
Available online 23 April 2017

Keywords:
Zinc
Mast cell
Hippocampus
Dentate gyrus
Timm stain
Sash mouse

ABSTRACT

The dentate gyrus of the hippocampus is a site of adult neurogenesis, and is also known to contain one of the highest concentrations of labile brain zinc (Zn), thought to aid in learning and memory by supporting neurogenesis. At the same time, it is known that unbound Zn, when present at excessive levels, decreases the formation of new neurons. Since mast cells contain Zn transporters capable of moving this essential element across their plasma membrane, as well as Zn-rich granules that are dispelled upon secretion, we reasoned that mast cells contribute to Zn homeostasis in this area of the brain, as they are found in greatest numbers in and around the dentate gyrus. This line of evidence was tested by comparing Timm-stained hippocampal sections of mast cell-deficient C57BL/6-*Kit*$^{W-sh/W-sh}$ (Sash$^{-/-}$) mice to those of mast cell-containing wild type (Sash$^{+/+}$) animals. Mast cell deficient mice were found to have significantly increased Timm-positive staining as compared to controls, reflecting an increase in labile or bioactive Zn in this region. As we observed no change in total brain Zn (protein-bound plus unbound Zn), these increases indicate that mast cells may serve to bind what would otherwise be excessive or deleterious levels of labile Zn, or that they are able to recruit metallothionein proteins. Because elevated levels of labile Zn are observed in the brains of patients with neurodegenerative diseases such as Alzheimer's, the potential contribution of mast cells to these diseases remains a compelling one. Overall, these data support a role for mast cells in either establishing or maintaining Zn homeostasis in the brain in the service of health, while Zn dysregulation has the potential to reduce learning, memory, and ultimately organismal survival.

1. Introduction

Zinc (Zn) is an essential nutrient crucial for the maintenance of cell homeostasis, abundantly present in all cells and life [1]. Although Zn is not toxic *per se* [2], animals are known to be sensitive to its depletion or excess, where the body responds in varied deleterious ways, including through growth retardation, immunodeficiency, and neuronal degeneration [3,4]. While hundreds of enzymes, transcription factors and signaling molecules depend on Zn [5], the full range of function of this trace metal remains undis-

Abbreviations: Aβ, amyloid β peptide; AD, Alzheimer's disease; Astr, amygdalostrial transition area; BBB, blood-brain barrier; BL, basolateral amygdala; c48/80, compound 48/80; CPu, caudate putamen; Den, dorsal endopiriform nucleus; DG, dentate gyrus; GI, gastrointestinal; LaDL, later dorsolateral amygdala; LaVL, lateral ventrolateral amygdala; NSD, no significant difference; OD, optical density; Sash$^{-/-}$, C57BL/6-*Kit*$^{W-sh/W-sh}$; WT, wild type; Zn, zinc.

* Corresponding author at: Department of Psychology, Columbia University, New York, NY, USA.
E-mail addresses: rhk2117@columbia.edu (R.H. Kennedy), aw2868@barnard.edu (A. Wiqas), jc3181@columbia.edu (J.P. Curley).

http://dx.doi.org/10.1016/j.neulet.2017.04.037

covered for immune cells like mast cells, which reside in every vascularized tissue studied [6–10], and are normally found on the brain side of the blood-brain barrier (BBB) [11], or can cross the BBB to the diencephalon, hippocampus, and leptomeninges [12–15].

In recent years, mast cells have been cast as more than main effector cells in allergies and asthma, and more than simple aids in host defense against pathogens. Beyond these well established roles, they are sensitive sensors and effectors of communication across the vascular, immune, and nervous systems. Indeed, they are sensitive to hormonally active chemicals and toxicants [16,17], are remarkable contributors to neuropsychiatric states such as anxiety [18], and are able to modulate neuroinflammation, which may contribute to diseases, such as Alzheimer's [19–23].

Mast cell effects can be traced back to the composition of their cytoplasmic granules, which may house a variety of mediators, including biogenic amines such as histamine and serotonin, cytokines, enzymes, ATP, neuropeptides, growth factors, lipid metabolites such as leukotrienes and prostaglandins, and heparin [23–26]. Their specific mediator content depends on their location, as they mature in tissues and respond to local factors after leaving the bone marrow. Overall, preformed granular material is released in minutes, while *de novo* materials are secreted within hours; together, these responses catalyze or amplify molecular and cellular responses throughout the body [27].

Along with proinflammatory molecules, it has long been known that mast cells are rich in Zn. Early electron microscopy studies putatively indicated a structural role for Zn inside cytosolic granules—stabilizing histamine-heparin complexes [28,29]. Histamine is a potent arbiter of allergic reactions in the body, and also plays a valuable role as a neurotransmitter in the central nervous system [30]. However, recent mechanistic studies of human mast cells indicate that Zn can also be released from signaling cascades that are distinct from those resulting in histamine release [31].

The brain contains one of the highest levels of Zn in the body. The majority of Zn (90%) is tightly bound to protein [32], including enzymes involved in numerous cellular signaling pathways [33]. Bound Zn is known to escape visualization by standard histochemical techniques like Timm staining or *N*-(6-methyl-8-quinolye)-*para*-tolurnesul-fonamide (TSQ) fluorescence [4,34,35]. Instead, these techniques are sensitive detectors of Zn that is not bound or is loosely bound to proteins; this Zn pool is interchangeably referred to as labile, chelatable, or "bioactive" (and also erroneously referred to as "free").

Labile brain Zn is largely found in specific synaptic vesicles in a subgroup of glutamatergic neurons and is released from synaptic vesicles during signaling [36–39]. Direct Zn signaling effects have been documented, particularly on NMDA and GABA receptors [37]. Labile Zn is important for spatial learning and memory, as it is necessary for the induction of long-term potentiation [40,41]. Moreover, in a basal state, mast cells are in their greatest numbers in and around the hippocampal formation, an area with the highest Zn concentrations detected in the mossy fiber-CA3 region [37].

The hippocampal formation is impressive on at least two major fronts: one, neurogenesis (i.e., the formation of new granule cells) persists into adulthood, and, two, many of its inputs are known to be unidirectional to affect spatial and declarative memory. These features come together in the dentate gyrus (DG) of the hippocampus, which is considered the first step to processing information that leads to episodic memory. The entorhinal cortex supplies a major input into the DG through fibers of the perforant pathway [42], yet the DG does not return this projection, but instead relays to the CA3 field of the hippocampus. At present, it is unknown what these specific processing patterns mean for the production of declarative memory.

Considering the fast-acting release of mast cell granule contents, the presence of Zn transporters poised to command its uptake and efflux [43], and localization of mast cells to a neuroanatomically distinct, Zn-rich region of the brain, we reasoned that mast cells might contribute to maintaining Zn homeostasis in the brain, demonstrating an additional vital function for these immune cells in vivo. To explore this possibility, we compared histochemically reactive Zn and total brain Zn present in the brains of mast cell normal and mast cell knockout mice, and measured the size of their respective dentate gyri as a proxy for differential hippocampal function.

2. Material and methods

2.1. Animals

2.1.1. Animals

Mast cell deficient C57BL/6-*Kit*$^{W-sh/W-sh}$ (Sash$^{-/-}$) mice were originally obtained from The Jackson Laboratory (a9B6.Cg-*KitW sh*/HNihrJaeBsmJ, strain 5051; Bar Harbor, ME) and bred to establish a colony at the Columbia University animal facility. These mice were crossed with wild type C57BL/6 mice (The Jackson Laboratory) to generate heterozygous mice (C57BL/6-*Kit*$^{W-sh/+}$; Sash$^{+/-}$). Male homozygous Sash$^{+/+}$ (WT) and Sash$^{-/-}$ littermates from heterozygote crosses were used in these experiments. Genotypes were determined by observing coat color, as the *Kit*$^{W-sh}$ mutation causes abnormalities in pigmentation [44]. Litters were weaned at 28 days, and animals were sacrificed at 4–8 weeks old. Except in the case of amygdala staining (n = 4), all comparisons and statistics used an n of 6 per genotype.

2.1.2. Housing

Mice were housed 2–5 per cage in transparent plastic bins (36 cm × 20 cm × 20 cm) in a room kept on a 12:12 light−dark cycle at 22 ± 1 °C. Cages had corn cob bedding (Bed-o'cobs, Maumee, OH), and food and water were provided *ad libitum*. All procedures were approved by the Institutional Animal Care and Use Committee at Columbia University.

2.1.3. Diet

Weaned animals were given free access by wire feeder to LabDiet (St. Louis, MO), which contained 85 ppm Zn as described in www.labdiet.com/cs/groups/lolweb/@labdiet/documents/web_content/mdrf/mdi4/~edisp/ducm04_028021.pdf.

2.2. Visualizing labile Zn in the brain

2.2.1. Perfusion

Animals were deeply anesthetized and perfused transcardially with freshly made perfusate solution from a Rapid TimmStain Kit (FD NeuroTechnologies, Columbia, MD). This kit tightly controls overfixation, further standardizing the Timm method [45]. Perfusate contained sodium sulfide and formaldehyde, which was immediately followed by an equal volume of freshly made 4% paraformaldehyde in 0.1 M phosphate buffer (PB), pH 7.4. Following perfusion, brains were extracted and postfixed overnight in 4% paraformaldehyde.

2.2.2. Harvesting brain sections

Post-fixed brains were blocked by removing the hindbrain and the most anterior portion of the forebrain, and cryoprotected in a series of sucrose gradients (10%, 20%, 30%), each for 48 h. Brains were stored in 30% sucrose for up to one week at 4 °C, or stored for up to a month at −80 °C before thawing and sectioning. Coronal sections (30 μm thick) were cut using a cryostat (Microm HM 500 M, Walldorf, Germany) and every fourth section was collected by thaw mounting onto gelatin-coated microscope slides (Probe-on-plus slides; FisherBrand, Waltham, MA). Importantly, every slide contained sections from both experimental groups (i.e., WT and

Sash$^{-/-}$) at similar Bregma coordinates ensuring that sections from comparison groups were processed identically for Timm staining intensity. Slides were left to dry overnight, and extra sections (i.e., every third and fourth section) stored at −20 °C until used in the study.

2.2.3. Zn staining

Reactive (labile) Zn was processed and visualized using a Rapid TimmStain Kit following manufacturer's instruction. Accordingly, all glassware, including staining jars, were thoroughly cleaned and rinsed with freshly distilled water (Milli-Q; EMD Millipore, Billerica, MA); no metal tools were used, as they could have produced staining artifacts. Four slides were processed simultaneously.

Once dried, slides were washed in 0.1 M PB (three times, for three min each) using clean glassware, before transferring to plastic slide tubes (Arrayit Corporation, Sunnyvale, CA). The development of Timm stain is sensitive to both time and light. Following an incubation of 50 min in a light blocking, temperature-controlled environment, maintained by submersion in a 26 °C water bath, slides were removed from tubes, and transferred to clean glass dishes containing fresh Milli-Q water to stop the reaction. Every second section was counterstained with 0.1% cresyl violet for 5 min in the dark and destained by dipping in deionized water, before following the same sequence of ethanol dehydration steps as Timm's-only stained sections. Slides were cleared in CitriSolv (Decon labs, King of Prussia, PA) (3 × 5 min) and coverslipped in resinous mounting medium (Krystalon EMD Millipore, Billerica, MA).

2.2.4. Quantitative analysis of timm staining in hippocampus and amygdala by optical density

High resolution images were taken using a Nikon Eclipse E800 microscope (Nikon CO., Tokyo, Japan) fitted with a Q-imaging Retiga EXi, fast 1394 camera (Quantitative Imaging, Surrect, BC, Canada) and QCapture software (Quantitative Imaging). Images were taken at uniform magnification, brightness, and contrast settings. NIH Image J (1.45 v) software was used to measure the optical density of Timm staining in the brain using Timm-only stained sections. For the hippocampus (Bregma −1.91 mm to Bregma −3.51 mm), area measurements were used to calculate the average intensity of the Timm stain, which can vary from light brown to black, reflecting increasing amounts of Zn in this region. A similar strategy was employed for quantification of staining in the amygdala, but images were first converted to an 8-bit grayscale. Amygdala staining analysis contained an n of 4, as some sections were not suitable for ImageJ analysis. In both areas, measurement of the areas was performed by observers blind to genotype. To determine statistical significance, a comparison of means between WT and Sash$^{-/-}$ was made using an unpaired two-tailed *t*-test in Prism software (GraphPad Software, La Jolla, CA).

2.3. Volumetric analysis

The volumes of the hilar region and the granule cell layer of the dentate gyrus were estimated using the Cavalieri method [46] in Sash$^{-/-}$ and WT mice. Using every fourth section, a two-dimensional area of the dentate gyrus was taken by measuring the area of cresyl violet-only stained sections in Image J by two separate individuals ($R^2 = 0.96$). The volume of each section was calculated by multiplying the area obtained from ImageJ (in μm^2) by the thickness of the section (30 μm) added to the distance between each measured section (90 μm). Total volume was then calculated by summing this volume across all sections, and an unpaired two-tailed *t*-test was performed in Prism (GraphPad) to compare mean volumes of these hippocampal areas between the two genotypes.

2.4. Measuring total Zn (labile and bound) in brain, heart, liver, and GI tract

To avoid Zn contamination due to leaching from glassware, surfaces and utensils were washed in dilute HCl and rinsed with distilled water prior to use. Animals were sacrificed and brains harvested and dissected before taking the heart, liver, and GI tract. Hippocampi and olfactory bulbs were viewed under stereotaxic microscope and dissected on top of blotting paper moistened with PBS to prevent tissue from slipping during dissection. The remainder of the brain was also taken, separate from these two areas. Next, liver, heart, and GI tract were removed and gently rinsed in ice-cold PBS to remove excess blood. After weighing samples, tissue was combined with EDTA-free lysis buffer (RIPA Lysis and Extraction Buffer, ThermoScientific, Grand Island, NY) in high-speed centrifugal conical tubes (SuperClear™ Ultra-High Performance Centrifuge Tubes, VWR, Radnor, PA) at a volume of 3 ml for every 1 g tissue, and sonicated (Omni international, Kennesaw, GA) in an ice bath. After centrifuging samples at 17,000 × *g* for 20 min, supernatant was transferred to clean tubes without disturbing the pellet.

Once collected, samples were processed for Zn using an absorbance-based quantification kit (Abcam, Cambridge, MA) with minor modification to manufacturer instruction. Briefly, aliquots of supernatant were combined with an equal volume of 7% TCA solution for a total volume of 120 μl, and centrifuged at the highest setting for 5 min to deproteinize. Aliquots of samples (60 μl) were run in duplicate in clear, flat-bottom polystyrene 96-well plates (Corning Costar, Fisher Scientific, Pittsburgh, PA); for each experiment, sample wells were selected non-systematically in order to avoid plate and edge effects. Plates were read once the reaction completed, which was determined in several experiments to be after an incubation of 10 min. Optical density at 570 nm was measured in a microplate reader (BioRad, Hercules, CA) using Microplate manager software 5.2.1 (BioRad). Zn levels in sample plate wells were calculated on the basis of a standard curve processed on the same plate, which included an expanded range of concentrations below 2 nM in order to obtain greatest sensitivity. Total Zn (μM) is reported on the basis of the sample readings paired to the organ mass of each animal.

3. Results

3.1. Mast cell deficient mice stain more intensely for labile Zn in brain

Mast cell deficient Sash$^{-/-}$ mice stained most intensely for labile Zn as compared to wild type littermate controls (Fig. 1). Visual inspection (Fig. 1a) and quantitative measurement (Fig. 1b–c) indicate that these differences are maintained throughout all coronal sections of the DG, with greater than 3.5 times the amount of Timm-positive staining appearing in mast cell deficient animals (i.e., compare Sash$^{-/-}$ OD of 1.44 ± 0.28 to WT OD of 0.65 ± 0.20 [mean ± SE]; $p = 0.0397$). When considered rostrally versus caudally, (Fig. 1c), significant labile Zn staining appears in both the rostral and dorsal aspects of the DG (rostral comparison of 1.36 ± 0.30 OD [Sash$^{-/-}$] versus 0.46 ± 0.15 OD [WT], mean ± SE, $p = 0.0246$; caudal comparison of 1.49 ± 0.28 [Sash$^{-/-}$] versus 0.54 ± 0.13 [WT], mean ± SE, $p = 0.0109$).

Moreover, Timm-positive staining differences were significant in brain regions relevant to learning and memory processes outside the hippocampus such as the amygdala (Fig. 2); Sash$^{-/-}$ OD of 2.47 ± 0.45, WT OD of 0.77 ± 0.25 (mean ± SE), $p = 0.0165$.

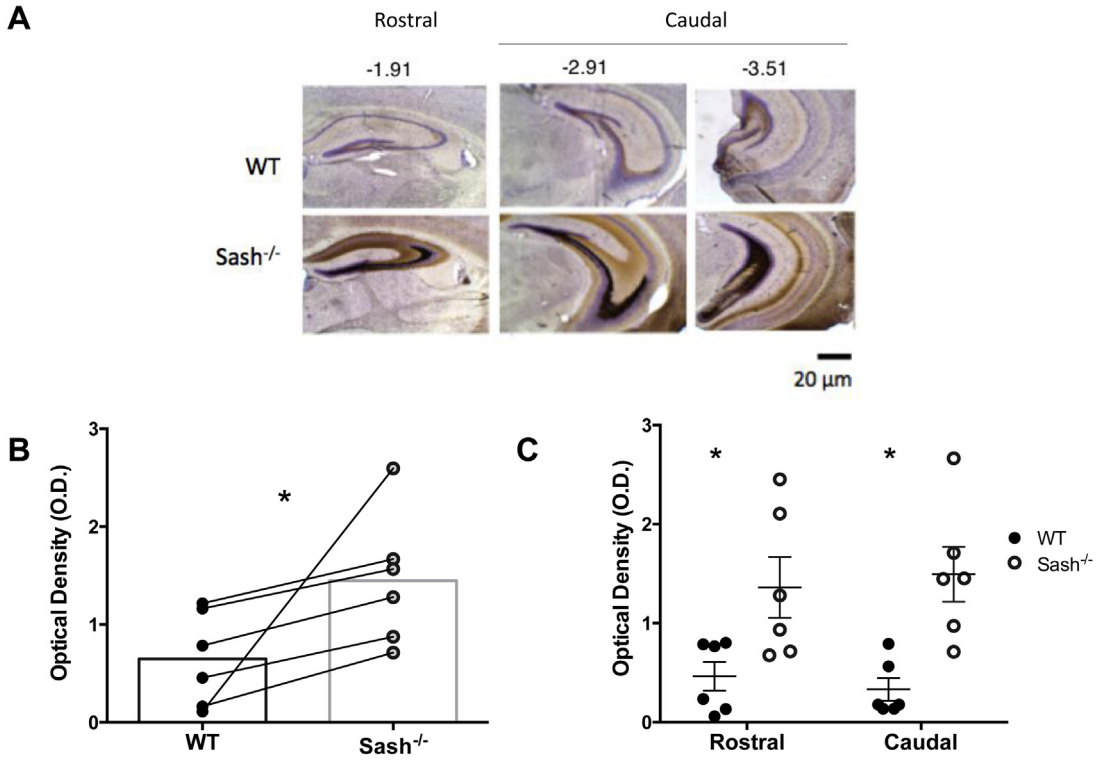

Fig. 1. Comparison of labile Zn staining along the rostral-caudal axis of hippocampus.
(A) Representative Timm staining (with cresyl violet counterstain) from Bregma −1.91, −2.91, and −3.51 mm in WT (top panel) and Sash$^{-/-}$ (bottom panel). Increasing intensity of Timm stain appears on a spectrum of light brown to black, which corresponds to relative increases in labile Zn. Coronal sections of perfused brains were mounted to a given slide containing with one animal per genotype and processed to control for variation in stain development as described in detail in the methods section.
(B) Quantification of Timm-positive staining by Image J, performed as reported in Methods. Symbols represent average staining from all given slices (−1.91 to −3.51 mm) of individual mice (n = 6 per genotype), and lines represent animals processed on the same slide. Statistical difference was determined by unpaired two-tailed *t*-test; *p = 0.0397.
(C) Optical density by position in the DG. Average OD for rostral and caudal DG are compared (Bregma −1.91 versus −2.91 and −3.51 combined). Each symbol represents an individual mouse (n = 6 per genotype); horizontal bars represent averages per group, and error bars are SD. Statistically significant staining differences between WT and Sash$^{-/-}$ were found at both the rostral and caudal areas of the DG, as determined by unpaired two-tailed *t*-tests (p = 0.0246, p = 0.0109, respectively.)

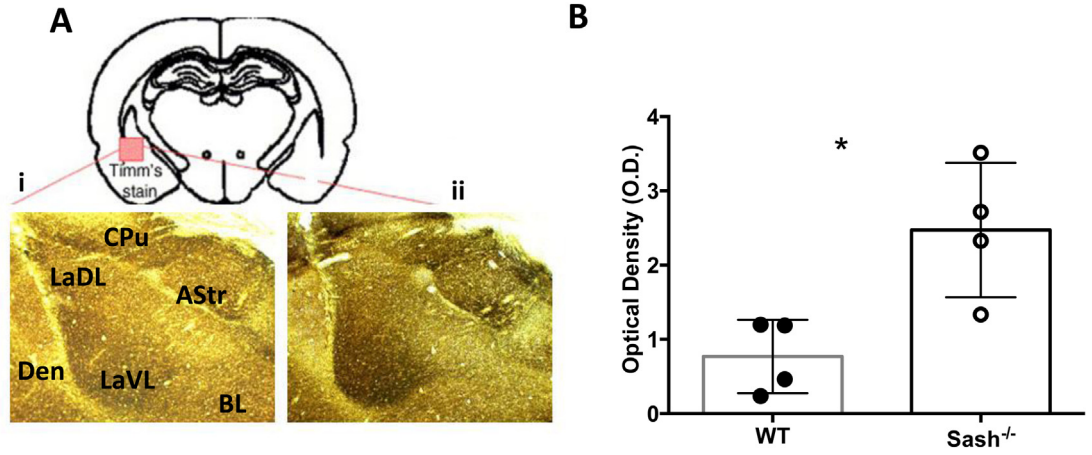

Fig. 2. A. Representative Timm-positive stain in the amygdala in (i) WT and (ii) Sash$^{-/-}$ mice and B. Quantification of Timm-positive staining. Perfused animals (n = 4) were stained for metal deposition as described in materials and methods. LaDL, later dorsolateral amygdala; LaVL, lateral ventrolateral amygdala; BL, basolateral amygdala; Astr, amygdalostrial transition area; CPu, caudate putamen; Den, dorsal endopiriform nucleus. *p = 0.0165, unpaired two-tailed *t*-test.

3.2. No significant difference in total Zn between WT and Sash$^{-/-}$

All mice in this study were fed the same diet and were the same approximate age and mass at sacrifice (data not shown) controlling for artificial Zn differences between genotypes. As shown in Fig. 3, NSD ($p > 0.05$) was detected between these animals in the whole brain, hippocampus, or olfactory bulb, another brain region known to be relatively high in brain Zn. Total Zn in liver, GI tract, and heart were also surveyed to understand possible metabolic partitioning of total Zn in the event that discrepancies were found in the brain; NSD were found in these organs.

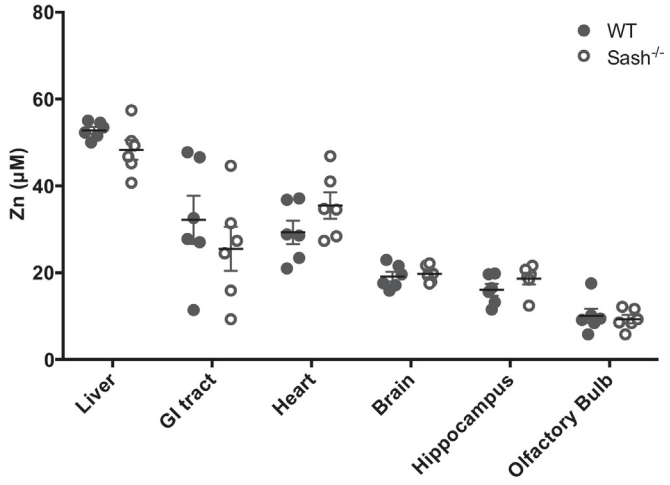

Fig. 3. Total Zn (bound and unbound) in selected tissue of the brain and body. Total Zn quantified by an absorbance assay as detailed in Material and Methods. Each data point represents an individual animal (n = 6); bars represent mean ± SEM. NSD as determined by multiple unpaired two-tailed *t*-tests performed between genotypes ($p > 0.05$).

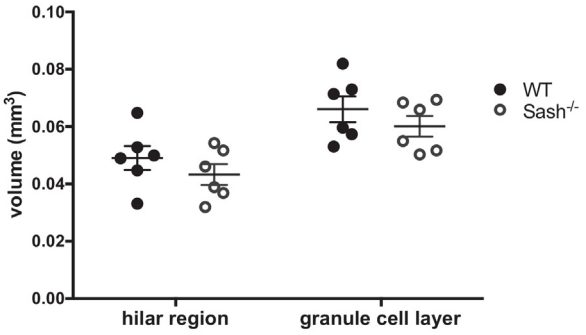

Fig. 4. Volumetric analyses of hilar region and granule cell layer of the DG. Analyses were based on Image J measurements as described in Material and Methods section. NSD ($p > 0.05$) as determined by unpaired two-tailed *t*-test.

3.3. No volumetric difference in dentate gyrus between mast cell deficient and WT mice

As depicted in Fig. 4, there was no detectable difference between mast cell deficient Sash$^{-/-}$ mice and WT controls, in the hilar region ($p = 0.7792$) or the granule cell layer ($p = 0.5415$) of the DG by unpaired two-tailed *t*-test.

4. Discussion

This study is the first to investigate Zn differences in the brains of mice known to have different levels of brain-resident mast cells. Here we report a significant increase in labile Zn in Sash$^{-/-}$ mouse brain, which occurs without altering total Zn levels. We reason that a reduced Timm-positive stain in mast cell-normal (WT) animals supports the idea that these immune cells modulate Zn availability either by recruiting metallothionein or by removing chelatable Zn through cellular incorporation. On the basis of these data, we may now begin to appreciate that mast cell degranulation also allows for the release of Zn back into the local milieu where it can be mobilized or bound. Overall, increased Zn staining in mast cell deficient (Sash$^{-/-}$) mice, uncovers for the first time a specific role of mast cells in biometal availability.

The Sash$^{-/-}$ mouse is a genetic mast cell loss-of-function in an animal that has *c-kit*-related phenotypic abnormalities but otherwise has a normal immune cell profile [47,48]. This suggests that mast cell degranulation, which can be triggered by environmental stimuli on the order of minutes [49], can modulate Zn homeostasis. Additionally, as mast cells are known to degranulate in response to otherwise innocuous stimuli, this points to an overlooked, but potentially important Zn-related pathological role for hyperresponsive brain mast cells. Functional studies that record Zn before and after manipulation of the degranulation state of mast cells, such as before and after intracerebroventricular injection of c48/80, are required to further reveal the sensitivity and reactivity of mast cells to regulating Zn in their local environment. These future studies will also serve to confirm the finding within our mast cell knockout model.

Zn, iron, and other first row transition metals are important in neuronal function and aging; accordingly, increasing evidence points to homeostatic dysfunction of biometals across several different types of neurodegenerative disease [50–52]. In AD, for example, there is growing evidence that endogenous metal ions such as Zn, iron, and copper can contribute to the aggregation of amyloid β peptide (Aβ) by binding to histidine residues within them [53]. Metal binding promotes aggregation of toxic self-propagating proteins, either leading to neurodegeneration [54–56], or may be neuroprotective [57]. Additionally, alteration of Zn transporters is consistently detected in mouse models and in AD human brain. Altogether, this evidence points to the real possibility that disruption of brain Zn homeostasis contributes to the pathological progression of AD [41].

Since mast cells are present in the brain throughout development and adulthood [14], mast cell Zn uptake, and release, may have lifelong contributions to the normal brain. With a reduction in mast cell numbers due to normal aging [58], we would also expect altered Zn homeostasis in the brain. Moreover, influx of mast cells across the BBB due to disease or infection has the potential to alter Zn availability and hence transcriptional and cellular signaling pathways that aid in repair, development, and growth of hippocampal neurons.

At this time, we understand the mast cell modulation of available brain Zn to be orchestrated either through cellular incorporation (via Zn transporters), or through the recruitment of metallothioneins (MTs). MTs are small cysteine-rich metalloproteins that are currently classified in 15 families [59]. They are known to play multiple roles, including in Zn and copper homeostasis, serving to protect against heavy metal toxicity in the brain [60,61].

Strain differences in Timm-stained mouse hippocampal sections have previously been reported [60], but not for our mast cell genotypes. Disorganization of cell layers, particularly in terminal projections of the mossy fiber region, have been reported for BALB/c, C57 B and Reeler mutant mice [62]. One of the hypotheses for these aforementioned strain differences has been suggested to be due to altered thyroid hormone levels, which can modify the formation of granule cells and the size of projections in the mossy fiber area [63,64]. Conversely, the genotype differences reported here do not reflect differences in connectivity in the dentate gyrus, but rather reflect levels of available Zn in these areas due to differences in mast cell numbers.

In this study, we report increased Timm-positive staining in all areas of the brain where labile Zn is known to reside. The most intense staining was found in learning-associated areas that include the amygdala, entorhinal cortex, and hippocampal formation, regardless of whether these brains belonged to mast cell deficient or mast cell normal mice. As in the hippocampus, Zn is known to be contained in synaptic boutons of both the amygdala and cortex [65,66]. The reason why Zn is enriched in certain neuronal vesicles is not completely understood, but is nevertheless

universally observed—all Zn-containing neurons are glutamatergic, but not all glutamatergic neurons are Zn-containing [66].

While brain Zn is known to be distributed across several compartments, and greatest pockets appear in areas appreciated for their roles in learning and memory, it was not necessarily anticipated that these areas would also be relatively intensely stained. These observations correspond nicely to behavioral differences our lab has previously observed for these genotypes (i.e., Sash$^{-/-}$ mice have impairments in spatial learning and memory as compared to mast cell normal heterozygotes in both radial arm and Morris water maze tests [58]). Since Fanselow and Dong report that the dorsal hippocampus performs mainly cognitive functions, while the ventral hippocampus relates to stress and emotion [67], we considered functional segregation of the hippocampus in our analysis of Timm-positive staining. These functionality differences do not affect the increased Zn staining in Sash$^{-/-}$ as compared to WT.

When interpreting these staining differences in regions outside the hippocampus, it is better to cast a wider net of appreciation: Timm stain in these areas is known to identify more than the single deposition of Zn, but to pick up other metals as well; on the other hand, it is universally understood that Timm-positive staining in the hippocampus is specific for Zn by default, given high levels of Zn found empirically in this area by several different methods [68]. Ongoing neurogenesis is essential to proper hippocampal functioning and the DG is one of three brain areas where new neurons are formed throughout life. The principal and most numerous cell of the DG is the granule cell of the mossy fiber pathway, which receives input from the entorhinal cortex [69]. In rats, the majority of granule cells are generated after birth [70].

We detected no difference in the size of the granule cell layer or hilus by cresyl violet staining. While a volumetric difference would have indicated impaired survival of neurons, and/or a decrease in progenitor cell proliferation, the fact that we have previously detected differences in granule cell layer with NeuN staining still points to this possibility, and underlines the importance of using littermates to reduce inherent variability [58].

It is well documented that brain mast cells add to neural histamine pools [71–73], and that lack of mast cell serotonin lends itself to anxiety-like behavior [18]. Modulation of available brain Zn may now be considered part of the mast cell repertoire for healthy brain function, along with the secretion of serotonin [74], contributing to proper hippocampal function, and learning and memory by association.

It will be important in future work to determine if the effect of mast cell degranulation and release of Zn has special status as compared to those in the periphery, especially with regard to neurological disorders. Although a causal relationship between mast cells and Zn has not been established here, these data support careful consideration of mast cell-related Zn effects, which may occur in response to degranulating agents that release mast cell granulocytic compartments.

Acknowledgements

We thank Drs. Rae Silver (Columbia University), Joe LeSauter (Barnard College), Kathryn Nautiyal (Columbia University), and Rachel Austin (Barnard College) for their generous aid and expertise. Funding for this work was provided by the College of Liberal Arts and Sciences at Columbia University (RK), The Arnold and Mabel Beckman Foundation, Beckman Scholars Award (AW), Barnard College Summer Research Institute (AW), and the Barnard College Program in Neuroscience (AW).

References

[1] C. Andreini, L. Banci, I. Bertini, A. Rosato, Zinc through the three domains of life, J. Proteome Res. 5 (2006) 3173–3178, http://dx.doi.org/10.1021/pr0603699.
[2] Agency for Toxic Substances and Disease Registry (ATSDR), Toxicological profile for Zinc. Atlanta, GA: U.S. Department of Health and Human Services, Public Health Service (2005).
[3] A.S. Prasad, Zinc and immunity, Mol. Cell. Biochem. (1998) 63–69, http://dx.doi.org/10.1023/A:1006868305749.
[4] J.Y. Koh, Zinc and disease of the brain, Mol. Neurobiol. 24 (99) (2001), http://dx.doi.org/10.1385/MN:24:1-3:099.
[5] J.E. Coleman, Zinc proteins: enzymes, storage proteins, transcription factors, and replication proteins, Annu. Rev. Biochem. 61 (1992) 897–946, http://dx.doi.org/10.1146/annurev.biochem.61.1.897.
[6] G. Brinkman, Mast cells in normal human bronchus and lung, J. Ultrastruct. Res. 23 (1968) 115.
[7] A.M. Dvorak, Mast-cell degranulation in human hearts, N. Engl. J. Med. 315 (1986) 969–970.
[8] I. Esposito, J. Kleeff, S.C. Bischoff, L. Fischer, P. Collecchi, M. Iorio, G. Bevilacqua, M.W. Buchler, H. Friess, The stem cell factor-c-kit system and mast cells in human pancreatic cancer, Lab. Invest. 82 (2002) 1481–1492, http://dx.doi.org/10.1097/01.LAB.0000036875.21209.F9.
[9] B. Hellstrom, H.J. Holmgren, Numerical distribution of mast cells in the human skin and heart, Acta Anat. (Basel) 10 (1950) 81–107.
[10] H.W. Steer, Mast-cells of human stomach, J. Anat. 121 (1976) 385–397.
[11] M. Khalil, J. Ronda, M. Weintraub, K. Jain, R. Silver, A.J. Silverman, Brain mast cell relationship to neurovasculature during development, Brain Res. 1171 (2007) 18–29, http://dx.doi.org/10.1016/j.brainres.2007.07.034.
[12] J.A. Kiernan, A comparative survey of the mast cells of the mammalian brain, J. Anat. 121 (1976) 303–311 http://www.pubmedcentral.nih.gov/articlerender.fcgi?artid=1231801&tool=pmcentrez&rendertype=abstract.
[13] R. Silver, A.-J. Silverman, L. Vitković, I.I. Lederhendler, Mast cells in the brain: evidence and functional significance, Trends Neurosci. 19 (1996) 25–31, http://dx.doi.org/10.1016/0166-2236(96)81863-7.
[14] A.J. Silverman, A.K. Sutherland, M. Wilhelm, R. Silver, Mast cells migrate from blood to brain, J. Neurosci. 20 (2000) 401–408.
[15] F. Florenzano, M. Bentivoglio, Degranulation, density, and distribution of mast cells in the rat thalamus: a light and electron microscopic study in basal conditions and after intracerebroventricular administration of nerve growth factor, J. Comp. Neurol. 424 (2000) 651–669.
[16] R.H. Kennedy, J.H. Pelletier, E.J. Tupper, L.M. Hutchinson, J.A. Gosse, Estrogen mimetic 4-tert-octylphenol enhances IgE-mediated degranulation of RBL-2H3 mast cells, J. Toxicol. Environ Health A 75 (2012) 1451–1455, http://dx.doi.org/10.1080/15287394.2012.722184.
[17] R.K. Palmer, L.M. Hutchinson, B.T. Burpee, E.J. Tupper, J.H. Pelletier, Z. Kormendy, A.R. Hopke, E.T. Malay, B.L. Evans, A. Velez, J.A. Gosse, Antibacterial agent triclosan suppresses RBL-2H3 mast cell function, Toxicol. Appl. Pharmacol. 258 (2012) 99–108, http://dx.doi.org/10.1016/j.taap.2011.10.012.
[18] K.M. Nautiyal, A.C. Ribeiro, D.W. Pfaff, R. Silver, Brain mast cells link the immune system to anxiety-like behavior, Proc. Natl. Acad. Sci. U. S. A. 105 (2008) 18053–18057, http://dx.doi.org/10.1073/pnas.0809479105.
[19] R. Kennedy, R. Silver, Neuroimmune signaling cytokines and the CNS, in: D.W. Pfaff, N.D. Volkow (Eds.), Neurosci. 21 st Century, Springer, 2016, pp. 1–41, http://dx.doi.org/10.1007/978-1-4614-6434-1_174-1.
[20] J. Kalesnikoff, S.J. Galli, New developments in mast cell biology, Nat. Immunol. 9 (2008) 1215–1223, http://dx.doi.org/10.1038/ni.f.216.
[21] S.D. Skaper, L. Facci, P. Giusti, Neuroinflammation, microglia and mast cells in the pathophysiology of neurocognitive disorders: a review, CNS Neurol. Disord. Drug Targets 13 (2014) 1654–1666, http://dx.doi.org/10.2174/1871527313666141130224206.
[22] R. Silver, J.P. Curley, Mast cells on the mind: new insights and opportunities, Trends Neurosci. 36 (2013) 513–521, http://dx.doi.org/10.1016/j.tins.2013.06.001.
[23] M. Krystel-Whittemore, K.N. Dileepan, J.G. Wood, Mast cell: a multi-functional master cell, Front. Immunol. 6 (2016), http://dx.doi.org/10.3389/fimmu.2015.00620.
[24] A.M. Gilfillan, S.J. Austin, D.D. Metcalfe, Mast cell biology: introduction and overview, Adv. Exp. Med. Biol. 716 (2011) 2–12, http://dx.doi.org/10.1007/978-1-4419-9533-9_1.
[25] E.Z.M. da Silva, M.C. Jamur, C. Oliver, Mast cell function: a new vision of an old cell, J. Histochem. Cytochem. (2014), http://dx.doi.org/10.1369/0022155414545334.
[26] D.D. Metcalfe, D. Baram, Y.A. Mekori, Mast cells, Physiol. Rev. 77 (1997) 1033–1079.
[27] S.J. Galli, S. Nakae, M. Tsai, Mast cells in the development of adaptive immune responses, Nat. Immunol. 6 (2005) 135–142, http://dx.doi.org/10.1038/ni1158.
[28] E. Pihl, G.T. Gustafso, Heavy metals in rat mast cell granules, Lab. Investig. 17 (1967) 588-.
[29] M. Murphy, V. Haarstad, Molecular orbital studies of the mast cell zinc-histamine storage complex, Int. J. Quantum Chem. 8S1 (1974) 149–157.
[30] S. Nuutinen, P. Panula, Histamine in neurotransmission and brain diseases, Adv. Exp. Med. Biol. 709 (2010) 95–107, http://dx.doi.org/10.1007/978-1-4419-8056-4-10.

[31] K. Nakashima-Kaneda, A. Matsuda, H. Mizuguchi, T. Sasaki-Sakamoto, H. Saito, C. Ra, Y. Okayama, Regulation of IgE-dependent zinc release from human mast cells, Int. Arch. Allergy Immunol. (2013) 44–51, http://dx.doi.org/10.1159/000350359.
[32] C.J. Frederickson, M.A. Klitenick, W.I. Manton, J.B. Kirkpatrick, Cytoarchitectonic distribution of zinc in the hippocampus of man and the rat, Brain Res. 273 (1983) 335–339, http://dx.doi.org/10.1016/0006-8993(83)90858-2.
[33] B.L. Vallee, K.H. Falchuk, The biochemical basis of zinc physiology, Physiol Rev. 73 (1) (1993) 79–118.
[34] G. Danscher, Histochemical demonstration of heavy metals, Histochem. Cell Biol. (1981) 1–16, http://dx.doi.org/10.1007/BF00592566.
[35] C.J. Frederickson, E.J. Kasarskis, D. Ringo, R.E. Frederickson, A quinoline fluorescence method for visualizing and assaying the histochemically reactive zinc (bouton zinc) in the brain, J. Neurosci. Methods 20 (1987) 91–103, http://dx.doi.org/10.1016/0165-0270(87)90042-2.
[36] M.P. Cuajungco, G.J. Lees, Zinc metabolism in the brain: relevance to human neurodegenerative disorders, Neurobiol. Dis. 4 (1997) 137–169, http://dx.doi.org/10.1006/nbdi.1997.0163.
[37] M.P. Cuajungco, G.J. Lees, Nitric oxide generators produce accumulation of chelatable zinc in hippocampal neuronal perikarya, Brain Res. 799 (1998) 118–129, http://dx.doi.org/10.1016/S0006-8993(98)00463-6.
[38] C.J. Frederickson, J.-Y. Koh, A.I. Bush, The neurobiology of zinc in health and disease, Nat. Rev. Neurosci. 6 (2005) 449–462, http://dx.doi.org/10.1038/nrn1671.
[39] H.J. Wenzel, T.B. Cole, D.E. Born, P. a Schwartzkroin, R.D. Palmiter, Ultrastructural localization of zinc transporter-3 (ZnT-3) to synaptic vesicle membranes within mossy fiber boutons in the hippocampus of mouse and monkey, Proc. Natl. Acad. Sci. U. S. A. 94 (1997) 12676–12681, http://dx.doi.org/10.1073/pnas.94.23.12676.
[40] Y.M. Lu, F. a Taverna, R. Tu, C. a Ackerley, Y.T. Wang, J. Roder, Endogenous Zn(2 +) is required for the induction of long-term potentiation at rat hippocampal mossy fiber-CA3 synapses, Synapse 38 (2000) 187–197, http://dx.doi.org/10.1002/1098-2396(200011)38:2<187::AID-SYN10>3.0.CO;2-R.
[41] L. Li, Z. Wang, Disruption of brain zinc homeostasis promotes the pathological progress of Alzheimer's disease, Histol Histopathol. 31 (6) (2016) 623–627, http://dx.doi.org/10.14670/HH-11-737.
[42] S. Ramón y Cajal, Estructura del asta de Ammon y fascia dentata, Ann. Soc. Esp. Hist. Nat. 22 (1893).
[43] L.H. Ho, R.E. Ruffin, C. Murgia, L. Li, S.A. Krilis, P.D. Zalewski, Labile zinc and zinc transporter ZnT4 in mast cell granules: role in regulation of caspase activation and NF-kappaB translocation, J. Immunol. 172 (2004) 7750–7760, http://dx.doi.org/10.4049/jimmunol.172.12.7750.
[44] C.-C. Chen, M.A. Grimbaldeston, M. Tsai, I.L. Weissman, S.J. Galli, Identification of mast cell progenitors in adult mice, Proc. Natl. Acad. Sci. U. S. A. 102 (2005) 11408–11413, http://dx.doi.org/10.1073/pnas.0504197102.
[45] C. Lopez-Garcia, E. Varea, J. Palop, J. Nacher, C. Ramierz, X. Ponsoda, A. Molowny, Cytochemical techniques for zinc and heavy metals localization in nerve cells, Microsc. Res. Tech. 56 (2002) 318–331.
[46] H. Gundersen, E. Jensen, The efficency of system sampling in stereology and its prediction, J. Microsc. 147 (1987) 229–263, http://dx.doi.org/10.1046/j.1365-2818.1999.00457.x.
[47] Y. Kitamura, J. Fujita, Regulation of mast cell differentiation, Bioessays 10 (1989) 193–196, http://dx.doi.org/10.1002/bies.950100604.
[48] M.A. Grimbaldeston, C.-C. Chen, A.M. Piliponsky, M. Tsai, S.-Y. Tam, S.J. Galli, Mast cell-deficient W-sash c-kit mutant Kit W-sh/W-sh mice as a model for investigating mast cell biology in vivo, Am. J. Pathol. 167 (2005) 835–848, http://dx.doi.org/10.1016/S0002-9440(10)62055-X.
[49] J. Kuby, Immunology, W.H. Freeman, New York, 1997.
[50] A.I. Bush, The metallobiology of Alzheimer's disease, Trends Neurosci. 26 (2003) 207–214, http://dx.doi.org/10.1016/S0166-2236(03)00067-5.
[51] S.S. Leal, H.M. Botelho, C.M. Gomes, Metal ions as modulators of protein conformation and misfolding in neurodegeneration, Coord. Chem. Rev. 256 (2012) 2253–2270, http://dx.doi.org/10.1016/j.ccr.2012.04.004.
[52] S. Pfaender, A.M. Grabrucker, Characterization of biometal profiles in neurological disorders, Metallomics 6 (2014) 960–977, http://dx.doi.org/10.1039/c4mt00008k.
[53] X. Huang, C.S. Atwood, R.D. Moir, M.A. Hartshorn, J.P. Vonsattel, R.E. Tanzi, A.I. Bush, Zinc-induced Alzheimer's A??1-40 aggregation is mediated by conformational factors, J. Biol. Chem. 272 (1997) 26464–26470, http://dx.doi.org/10.1074/jbc.272.42.26464.
[54] D. Noy, I. Solomonov, O. Sinkevich, T. Arad, K. Kjaer, I. Sagi, Zinc-amyloid β interactions on a millisecond time-scale stabilize non-fibrillar Alzheimer-related species, J. Am. Chem. Soc. 130 (2008) 1376–1383, http://dx.doi.org/10.1021/ja076282l.
[55] J. Danielsson, R. Pierattelli, L. Banci, A. Graslund, High-resolution NMR studies of the zinc-binding site of the Alzheimer's amyloid beta-peptide, FEBS J. 274 (2007) 46–59, http://dx.doi.org/10.1111/j.1742-4658.2006.05563.x.
[56] W.T. Chen, Y.H. Liao, H.M. Yu, I.H. Cheng, Y.R. Chen, Distinct effects of Zn2+, Cu2+, Fe3+, and Al3+ on amyloid-?? stability, oligomerization, and aggregation: amyloid-?? destabilization promotes annular protofibril formation, J. Biol. Chem. 286 (2011) 9646–9656, http://dx.doi.org/10.1074/jbc.M110.177246.
[57] P. Faller, C. Hureau, Bioinorganic chemistry of copper and zinc ions coordinated to amyloid-beta peptide, Dalton Trans. 108 (2009) 1080–1094.
[58] K.M. Nautiyal, Mast Cells Affect Hippocampal Physiology and Function, Columbia University, 2011.
[59] P.A. Binz, J.H.R. Kagi, Metallothionein Molecular evolution and classification, in: C. Klaassen (Ed.), Met. IV, Birkhauser Verlag AG, Basel, Switzerland, 1999, pp. 7–13.
[60] R. Deloncle, O. Guillard, J.L. Bind, J. Delaval, N. Fleury, G. Mauco, G. Lesage, Free radical generation of protease-resistant prion after substitution of manganese for copper in bovine brain homogenate, Neurotoxicology 27 (2006) 437–444, http://dx.doi.org/10.1016/j.neuro.2006.01.003.
[61] P. Adam, S. Krizkova, Z. Heger, P. Babula, V. Pekarik, M. Vaculovicoa, C.M. Gomes, R. Kizek, V. Adam, R. Kizek, V. Adam, Metallothioneins in prion-and amyloid-related diseases, J. Alzheimer's Dis. 51 (2016) 637–656, http://dx.doi.org/10.3233/JAD-150984.
[62] R. Barber, J.E. Vaughn, R.E. Wimer, C.C. Wimer, Geneticaly-associated variations in distribution of dentate granule cell synapses upon pyramidal cell dendrites in mouse hippocampus, J. Comp. Neurol. 156 (1974) 417–434, http://dx.doi.org/10.1002/cne.901560404.
[63] M.D. Madeira, M. Paula-Barbosa, A. Cadete-Leite, M.A. Tavares, Unbiased estimate of cerebellar granule cell numbers in hypothyroid and in sex-age-matched control rats, J. Hirnforsch. 29 (1988) 587–594.
[64] M. Blaabjerg, J. Zimmer, The dentate mossy fibers: structural organization, development and plasticity, Prog. Brain Res. 163 (2007), http://dx.doi.org/10.1016/S0079-6123(07)63005-2.
[65] N. Ichinohe, K.S. Rockland, Distribution of synaptic zinc in the macaque monkey amygdala, J. Comp. Neurol. 489 (2005) 135–147, http://dx.doi.org/10.1002/cne.20632.
[66] C.J. Frederickson, S.W. Suh, D. Silva, C.J. Frederickson, R.B. Thompson, Importance of zinc in the central nervous system: the zinc-containing neuron, J. Nutr. 130 (2000) 1471S–1483S http://jn.nutrition.org/content/130/5/1471S.short.
[67] M.S. Fanselow, H.-W. Dong, Are the dorsal and ventral hippocampus functionally distinct structures? Neuron 65 (2010) 7–19, http://dx.doi.org/10.1016/j.neuron.2009.11.031.
[68] D.G. Amaral, H.E. Scharfman, P. Lavenex, The dentate gyrus: fundamental neuroanatomical organization (dentate gyrus for dummies), Prog. Brain Res. 163 (2007), http://dx.doi.org/10.1016/S0079-6123(07)63001-5.
[69] C. Leranth, T. Hajszan, Extrinsic afferent systems to the dentate gyrus, Prog. Brain Res. 163 (2007), http://dx.doi.org/10.1016/S0079-6123(07)63004-0.
[70] S.A. Bayer, J. Altman, Hippocampal development in the rat: cytogenesis and morphogenesis examined with autoradiography and low-level X-irradiation, J. Comp. Neurol. 158 (1974) 55–79, http://dx.doi.org/10.1002/cne.901580105.
[71] A.J. Bugajski, Z. Chlap, J. Bugajski, J. Borycz, Effect of compound 48/80 on mast cells and biogenic amine levels in brain structures and on corticosterone secretion, J. Physiol. Pharmacol. 46 (1995) 513–522.
[72] R. Oishi, Y. Itoh, T. Fukuda, Y. Araki, K. Saeki, Comparison of the size of neuronal and non-neuronal histamine pools in the brain of different rat strains, J. Neural Transm. 73 (1988) 65–69, http://dx.doi.org/10.1007/BF01244623.
[73] R. Grzanna, L.D. Shultz, Ttion of mast-cells to the hustamine content of the central nervous system – a regional analysis, Life Sci. 30 (1982) 1959–1964, http://dx.doi.org/10.1016/0024-3205(82)90434-9.
[74] K.M. Nautiyal, C.A. Dailey, J.L. Jahn, E. Rodriquez, N.H. Son, J.V. Sweedler, R. Silver, Serotonin of mast cell origin contributes to hippocampal function, Eur. J. Neurosci. 36 (2012) 2347–2359, http://dx.doi.org/10.1111/j.1460-9568.2012.08138.x.